Supporting Information

Theoretical screening of graphyne-supported single transition metals for the N_2 reduction reaction

Min Li,[a] Qinglong Fang,[a, b, c, *] Xumei Zhao,[a, *] Caijuan Xia,[a, b, c] Anxiang Wang,[a] You Xie,[d] Fei Ma,[e,] Jianmei She,[f] Zhongxun Deng,[f]

[a] *School of Science, Xi'an Polytechnic University, Xi'an 710048, Shaanxi, China*

[b] *Engineering Research Center of Flexible Radiation Protection Technology, University of Shaanxi Province, Xi'an Polytechnic University, Xi'an 710048, Shaanxi, China*

[c] *Xi'an Key Laboratory of Nuclear Protection Textile Equipment Technology, Xi'an Polytechnic University, Xi'an 710048, Shaanxi, China*

[d] *College of Science, Xi'an University of Science and Technology, Xi'an, 710054, Shaanxi, China*

[e] *State Key Laboratory for Mechanical Behavior of Materials, Xi'an Jiaotong University, Xi'an 710049, Shaanxi, China*

[f] *Shenmu Vocational & Technical College, Shenmu, 719300, Shaanxi, China*

* Corresponding authors.

E−mail addresses: qinglong_fang@xpu.edu.cn (Qinglong Fang);

20191211@xpu.edu.cn (Xumei Zhao).

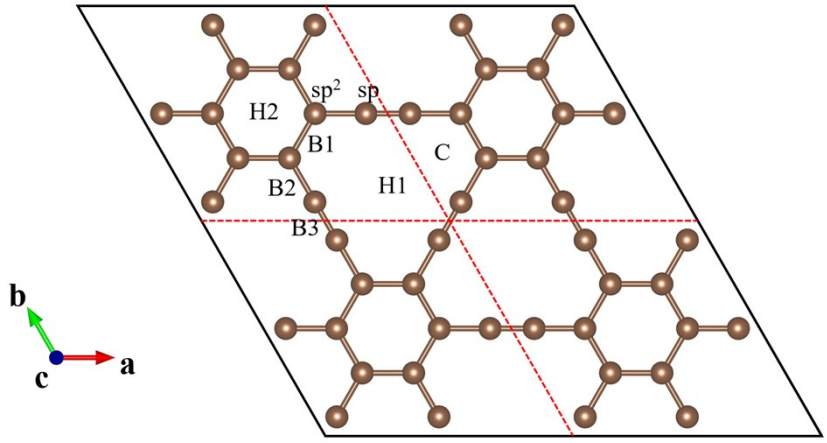

Fig. S1 The top vieww of the (2 × 2) GY supercell, which *sp*- and sp^2-hybridized C atoms coexist. The all possible adsorption sites of TM are labeled, i.e. B1, B2, B3, H1, H2, and C.

Table S1. The N-N bond length ($L_{N\text{-}N}$, Å) of N_2 adsorbed on TM@GY and the Bader charge (Q_{N2}, |e|) transfer between N and TM@GY.

TM@GY	End-on		Side-on	
	$L_{N\text{-}N}$ (Å)	Q_{N2} (e)	$L_{N\text{-}N}$ (Å)	Q_{N2} (e)
Sc@GY	**1.136**	**0.236**	**1.164**	**0.414**
Ti@GY	1.131	0.183	1.179	0.489
V@GY	**1.131**	**0.170**	**1.163**	**0.361**
Cr@GY	1.139	0.303	1.188	0.466
Mn@GY	**1.138**	**0.279**	**1.172**	**0.371**
Fe@GY	1.138	0.274	1.158	0.302
Co@GY	1.130	0.213	1.115	0.017
Ni@GY	1.115	0.014	1.115	0.019
Cu@GY	1.115	0.005	1.115	0.006
Y@GY	**1.141**	**0.351**	**1.165**	**0.480**
Zr@GY	1.130	0.185	1.180	0.563
Nb@GY	1.136	0.266	1.166	0.424
Mo@GY	1.149	0.362	1.194	0.490
Tc@GY	**1.150**	**0.377**	**1.203**	**0.449**
Ru@GY	1.144	0.324	1.174	0.334
Rh@GY	1.134	0.225	1.115	0.014
Pd@GY	1.115	0.010	1.115	0.011
Ag@GY	1.115	0.004	1.115	0.007
Hf@GY	1.135	0.189	1.189	0.559

Ta@GY	1.143	0.315	1.180	0.489
W@GY	1.158	0.462	1.211	0.587
Re@GY	1.158	0.414	1.226	0.542
Os@GY	**1.144**	**0.297**	**1.188**	**0.386**
Ir@GY	1.136	0.192	1.156	0.233
Pt@GY	1.115	0.010	1.115	0.011
Au@GY	1.115	0.005	1.115	0.005

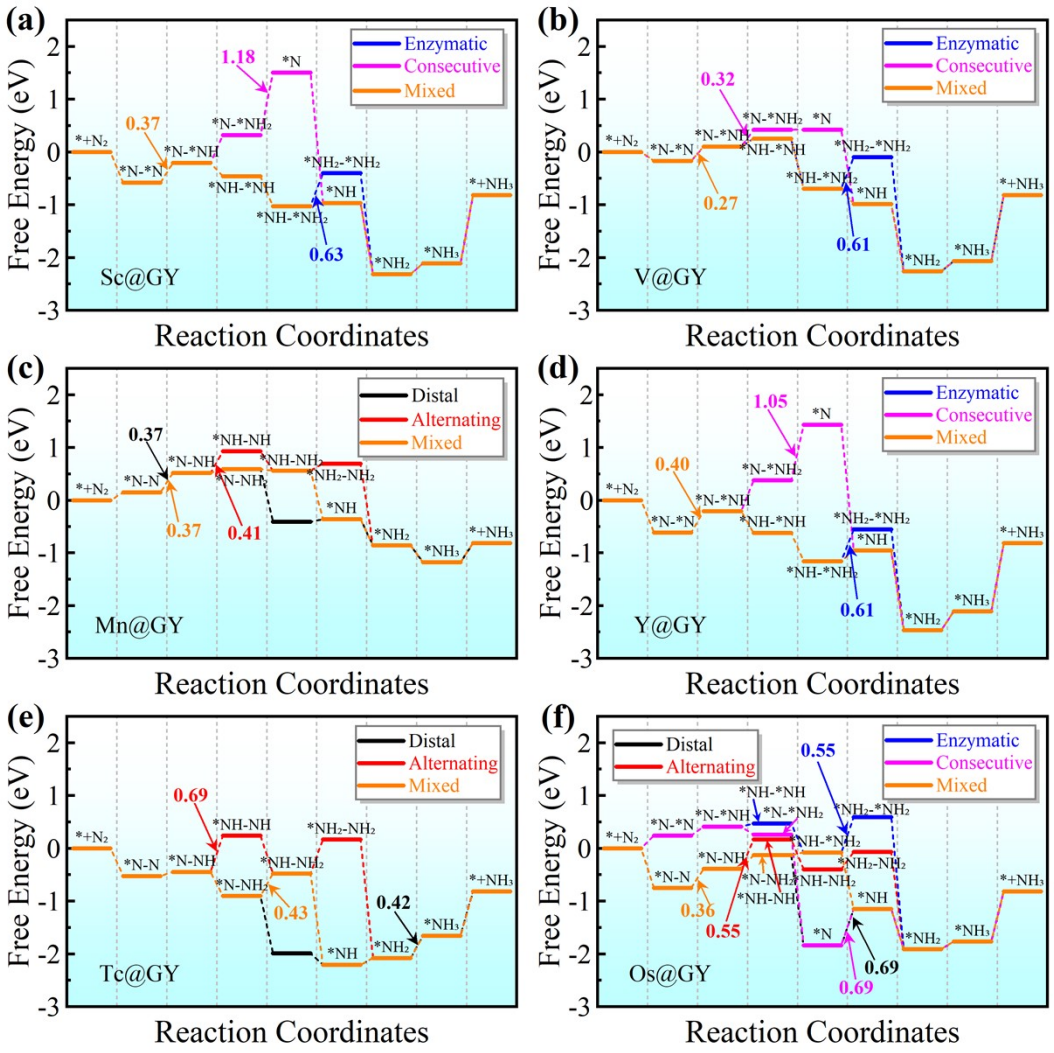

Fig. S2. NRR free energy diagrams of NRR on (a) Sc@GY, (b) V@GY, (c) Mn@GY, (d) Y@GY, (e) Tc@GY, and (f) Os@GY via the possible pathways.

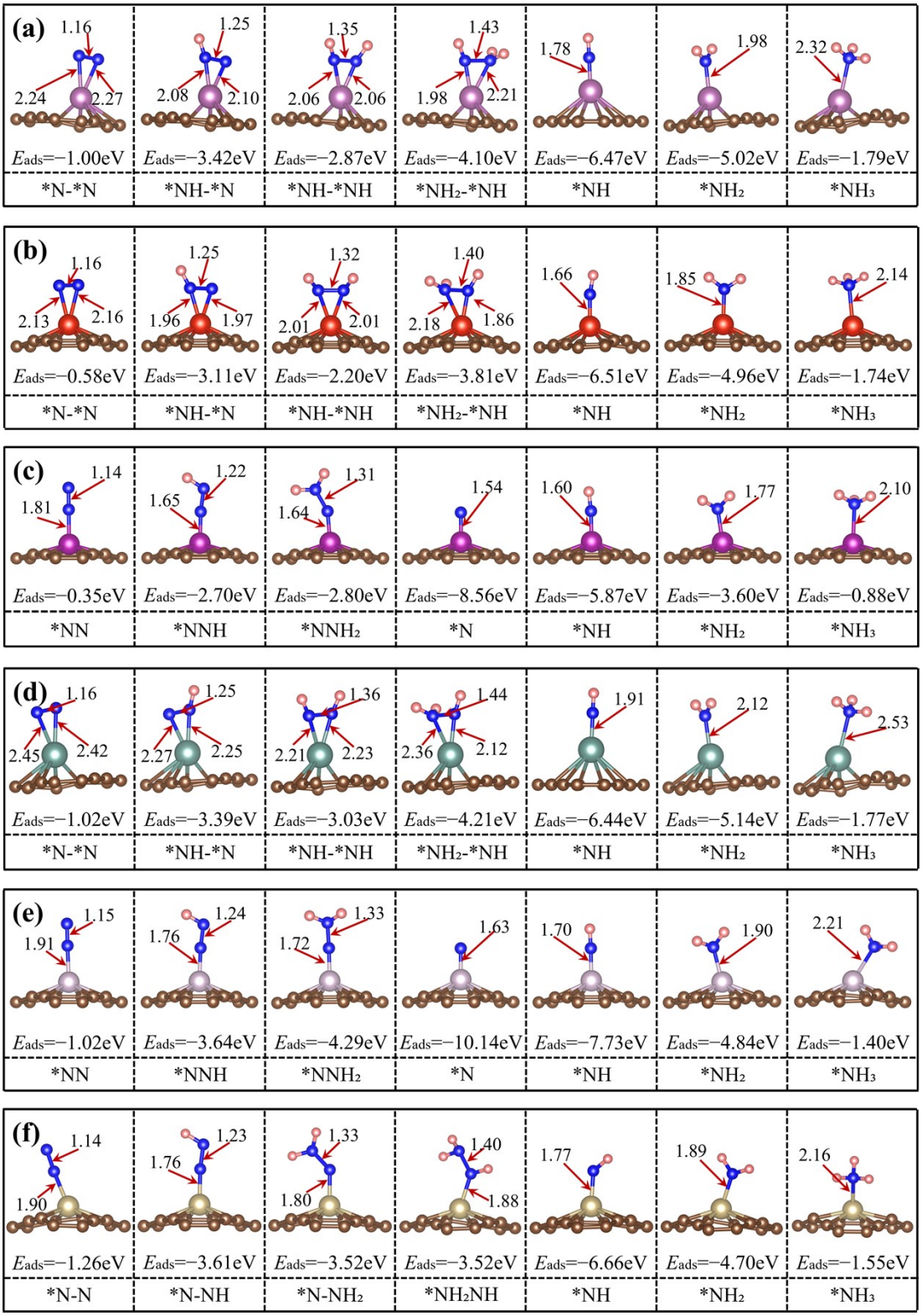

Fig. S3. Optimized Structures of the possible intermediates on (a) Sc@GY, (b) V@GY, (c) Mn@GY, (d) Y@GY, (e) Tc@GY, and (f) Os@GY via the most favorable pathway.

The corresponding E_{ads} and boYnd length of TM–N and N−N between the Candidate Catalyst and reaction intermediates are also displayed.

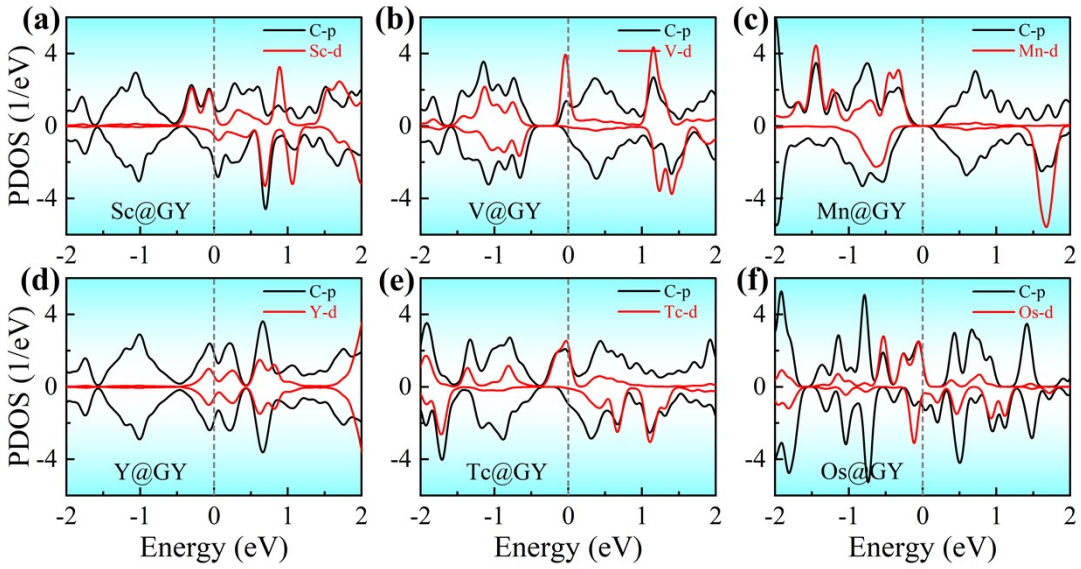

Fig. S4. The partial densities of states (PDOS) of (a) Sc@GY, (b) V@GY, (c) Mn@GY, (d) Y@GY, (e) Tc@GY, and (f) Os@GY. The Fermi level is set to zero and indicated by the dotted line.

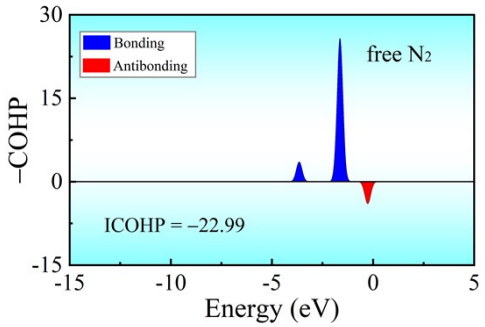

Fig. S5. The crystal orbital Hamilton populations (COHPs) of the N–N bond in a free N_2 molecule.

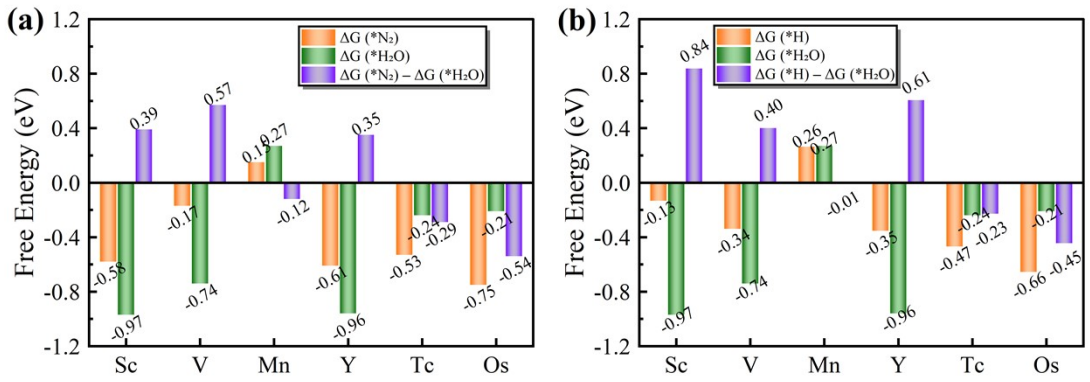

Fig. S6. Gibbs free energy of (a) $*N_2$ (ΔG_{*N2}) and $*H_2O$ (ΔG_{*H2O}), and the difference between them ($\Delta G_{*N2}-\Delta G_{*H2O}$) on Sc, V, Mn, Y, Tc, and Os@GY. (b) $*N_2$ (ΔG_{*H}) and $*H_2O$ (ΔG_{*H2O}), and the difference between them ($\Delta G_{*H}-\Delta G_{*H2O}$) on Sc, V, Mn, Y, Tc, and Os@GY.